Available online at www.sciencedirect.com
ScienceDirect
Trans. Nonferrous Met. Soc. China 20(2010) 2294−2298
Transactions of Nonferrous Metals Society of China
www.tnmsc.cn

Preparation, characterization and photocatalytic activity of sulfuric acid-modified titanium-bearing blast furnace slag

LEI Xue-fei(雷雪飞)[1], XUE Xiang-xin(薛向欣)[2]

1. Department of Materials Science and Engineering, Northeastern University of Qinhuangdao, Qinhuangdao 066004, China;
2. School of Materials and Metallurgy, Northeastern University, Shenyang 110819, China

Received 27 November 2009; accepted 14 March 2010

Abstract: The feasibility of reducing Cr(VI) from the aqueous solution by sulfuric acid-modified titanium-bearing blast furnace slag (SATBBFS) as a photocatalyst was investigated. The photocatalysts were examined by X-ray diffraction (XRD), UV-vis diffuse reflectance spectra, thermogravimetric analysis (TG) and Fourier transform infrared spectroscopy (FTIR). The photocatalytic activities of the different catalysts were evaluated by the photocatalytic reduction of Cr(VI) under UV-vis light irradiation. The results show that the photocatalytic activities of SATBBFS catalysts are strongly dependent on $CaTiO_3$-to-TiO_2 mass ratio, adsorption capacity and surface acidity, and SATBBFS calcined at 400 °C shows a higher photocatalytic activity compared with other catalysts.

Key words: titanium-bearing blast furnace slag; doping; photocatalytic reduction; Cr(VI)

1 Introduction

In China, there are more than three million tons of titanium-bearing blast furnace slag (TBBFS) produced by iron and steel industry each year. It is wasteful to dispose TBBFS containing about 20% TiO_2 as ordinary blast furnace slag through traditional re-utilization processes, such as preparation of dam concrete, nanocrystalline cast stone, stone canal and titanium-silicon[1]. To use these titanium resources in TBBFS more effectively and diminish the influence of TBBFS on environment deterioration, the whole of TBBFS as photocatalyst was proposed[2]. LEI and XUE[3] adopted high-energy ball milling technique at high temperature to get $TBBFS_{700}$ photocatalysts and concluded that the photocatalytic activity of $TBBFS_{700}$ reached 88% of that of P25 TiO_2 after 6 h. The obvious advantages of the whole of TBBFS as photocatalysts are the lower costs and easy to be isolated.

Cr(VI) is widely used in electroplating, metal finishing, chromate preparation, tannery and fertilizer industries[4−5]. But, it has been reported that Cr(VI) can contaminate surface and ground water. Recently, many reports on the photocatalytic degradation of organic pollutions and Cr(VI) by SO_4^{2-}/TiO_2 photocatalysts have been published[6−8]. Among them, it was generally accepted that the sulfation of TiO_2 improved the photocatalytic activity of catalyst. Moreover, few reports are available on the photocatalytic reduction of Cr(VI) by perovskite photocatalysts[3, 9]. In this study, perovskite type SATBBFS photocatalysts were firstly synthesized and the photo-reduction of Cr(VI) by these photocatalysts was also studied. This study will be greatly useful in our quest for a better technological condition to dispose solid waste and wastewater.

2 Experimental

2.1 Materials

TBBFS, from Panzhihua Iron and Steel Corporation, China, was used in this study. The composition of TBBFS has been reported elsewhere[5]. In the preparation of SATBBFS powder, massive TBBFS was broken into pieces; the resulting shatters were then comminuted by disintegrator; subsequently, the powder was prepared by mixing 5.0 g TBBFS powder with 13 mL 0.2 mol/L H_2SO_4 in the high-energy ball mill for

Foundation item: Project(N090423003) supported by the Basic Scientific Research Costs of Central Colleges of China; Project(2007CB613504) supported by the National Basic Research Program of China; Project(307009) supported by the Foundation for Key Program of Ministry of Education, China

Corresponding author: LEI Xue-fei; Tel: +86-335-8047521; E-mail: leixuefei69@163.com

DOI: 10.1016/S1003-6326(10)60643-7

96 h and followed by drying at 80 °C. After pulverizing, SATBBFS powders were calcined in air at a heating rate of 5 °C/min up to 400, 500, 600 and 700 °C and held for 2 h，then cooled down by nature. The resulting catalysts were labeled as SATBBFS$_x$, where x denoted the calcination temperature (°C). Titanium dioxide Degussa P25 was used as a reference and it was not pre-treated or modified before using in our experiments.

2.2 Characterization of SATBBFS$_x$ catalysts

The X-ray diffraction (XRD) patterns of SATBBFS$_x$ powders were obtained by using Philips X'pert X-ray diffractometer with Cu K_α radiation. Fourier transform infrared (FT-IR) spectrum was recorded on a Nexus−670 instrument. The optical reflectance spectra were recorded on a Shimazu UV−2500 spectrophotometer. The thermogravimetric analysis (TGA) was carried out on SDT 2960 Simultaneous DSC-TGA instrument, with a heating rate of 5 °C/min from room temperature to 800 °C in air atmosphere. The particle size distribution of prepared powder was gotten by using BT−1600 image analyzer.

2.3 Photocatalytic experiment of SATBBFS$_x$ catalysts

Photocatalytic irradiations were carried out in a recirculating reactor equipped with a quartz immersion well, 240 mm in length, 80 mm in inner diameter, where a 500 W medium-pressure mercury lamp was placed. The lamp emitted predominantly at 365–366 nm with smaller emissions at lower wavelengths and with a significant emission in the visible region. Catalyst suspension (1 000 mL) was continuously recirculated to the photoreactor from a glass reservoir by means of a peristaltic pump. The irradiated volume in the well was 200 mL. The whole setup was thermostatic at (25±3) °C. And the initial concentration of Cr(VI) solution was 20 mg/L. Prior to the photocatalytic experiments, suspensions were stirred in the dark to permit the adsorption/desorption equilibrium until the concentration of Cr(VI) solution was constant. The concentration of Cr(VI) after adsorption equilibration was taken as the initial concentration of the photocatalytic experiments, to discount changes in the dark. At regular intervals, a 10 mL aliquot of the suspension was withdrawn and centrifuged. Subsequently, the supernatant solution was analyzed for the remaining Cr(VI) at a wavelength of 540 nm on a UV–vis spectrophotometer by the diphenylcarbazide colorimetric method. The photocatalytic activity was evaluated by the reduction efficiency (η) of Cr(VI) after experiment.

$$\eta = \left((\rho_0' - \rho_t) \Big/ \rho_0' \right) \times 100\% \quad (1)$$

where ρ_0' is the initial concentration of Cr(VI) (mg/L) after adsorption equilibrium, ρ_t is the concentration of Cr(VI) (mg/L) at any time t, and η is the reduction efficiency of Cr(VI) .

3 Results and discussion

3.1 Crystal phase and morphography

The XRD patterns of SATBBFS$_x$ catalysts calcined at different temperatures are shown in Fig.1. It is obviously observed that the XRD patterns of SATBBFS catalysts are different from those of TBBFS catalysts[3], indicating that the surface inorganic modification to TBBFS has some effects on the crystalline phase. Through comparing XRD patterns of TBBFS$_x$ and SATBBFS$_x$ catalysts, we find that there appears a new crystalline phase (anatase) for all SATBBFS$_x$ catalysts. The anatase content increases slightly with the increment of the calcination temperature. It can be observed from Fig.2 that the calcination temperature influences the perovskite content of SATBBFS$_x$ catalysts. As the calcination temperature increases, the perovskite content of SATBBFS$_x$ catalysts presents fluctuations. Such a change in the perovskite content may be due to the influence of activation temperature. Increasing the calcination temperature above the activation temperature promotes the periodic circulation of the crystalline phases and surface species of catalysts, which accounts for the fluctuation of perovskite content of SATBBFS$_x$ catalysts[10]. The FTIR spectra of SATBBFS$_x$ catalysts calcined at different temperatures are given in Fig.3. The bands at 570 cm^{-1} correspond to the characteristic absorption peak of perovskite in the prepared samples, and 460, 963, 1 040 cm^{-1} correspond to the characteristic absorption peak of diopside, while 910 cm^{-1} corresponds to the characteristic absorption peak of pyrope-essonite[11].

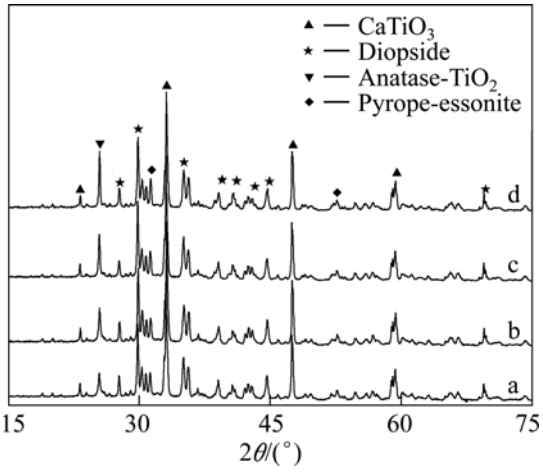

Fig.1 XRD patterns of SATBBFS$_{400}$ (a), SATBBFS$_{500}$ (b), SATBBFS$_{600}$ (c) and SATBBFS$_{700}$ (d)

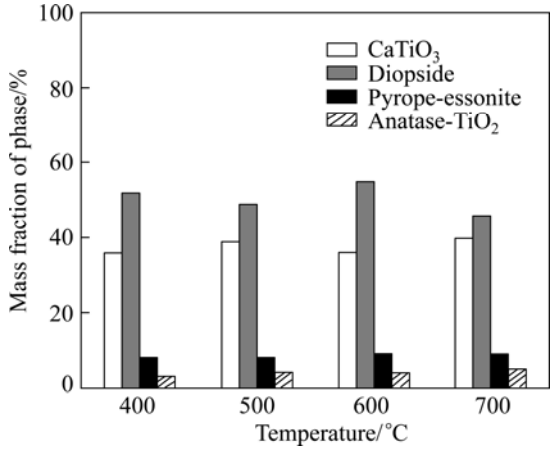

Fig.2 Phase mass fractions in SATBBFS$_x$ catalysts calcined at different temperatures

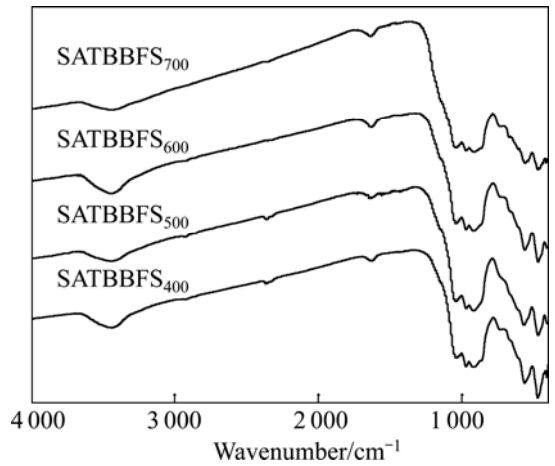

Fig.3 FTIR spectra of SATBBFS$_x$ catalysts calcined at different temperatures

For the broad strong peak of TiO_2 around 350 cm^{-1} exceeds the measurement range(399−4000 cm^{-1}), TiO_2 cannot be detected in our experiments. Based on the above analyses, it can be concluded that all SATBBFS catalysts are identified to be a mixture of perovskite, diopside, pyrope-essonite and TiO_2. The SEM images of SATBBFS$_x$ catalysts are similar with those reported in Ref.[10]. All the prepared samples display more and more serious aggregation with the increase of the calcination temperature.

3.2 UV–vis diffuse reflectance spectra

The UV–vis diffuse reflectance spectra of SATBBFS$_x$ catalysts and P25 TiO_2 are illustrated in Fig.4. The scanning wavelengths range from 240 to 800 nm. It is demonstrated that the increase in calcination temperature results in a slightly increase in UV-absorption capacity of the catalysts (especially for high temperature). Though P25 TiO_2 has stronger absorbability than SATBBFS powders calcined at various temperatures in the ultraviolet light region, the absorption region of SATBBFS powders extends to the invisible region. A significant increase in the absorption at wavelengths more than 400 nm indicates the decrease of band gap energies for SATBBFS$_x$ catalysts. The smaller band gap energy means a wider response range of catalysts, and the catalysts can absorb more photons[12]. This would contribute to an enhanced photocatalytic activity.

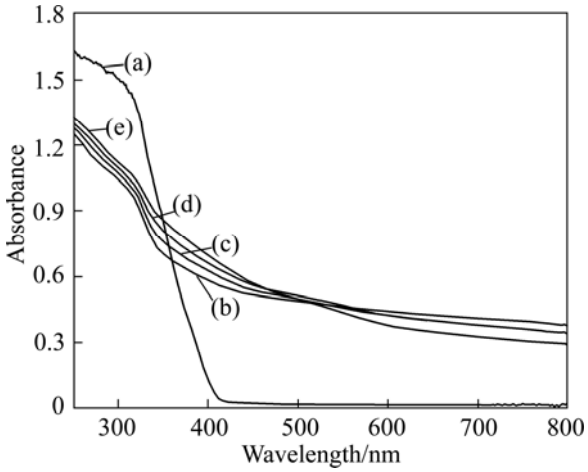

Fig.4 UV-vis diffuse reflection spectra for SATBBFS$_x$ powders calcined at different temperatures: (a) P25 TiO_2; (b) $SATBBFS_{400}$; (c) $SATBBFS_{500}$; (d) $SATBBFS_{600}$; (e) $SATBBFS_{700}$

3.3 TG analysis

Fig.5 shows the TGA curves of TBBFS and SATBBFS catalysts. As shown in Fig.5, the major mass loss of 1.5% between 35 and 500 °C is due to the dehydration of physically absorbed and crystallization water in TBBFS. In contrast, SATBBFS sample shows the mass loss in two stages. In the first stage (below 150 °C), aside from the evaporation of water, an additional mass loss occurs corresponding to sulfate oxoanions decomposition. Between 150 and 500 °C, the mass loss

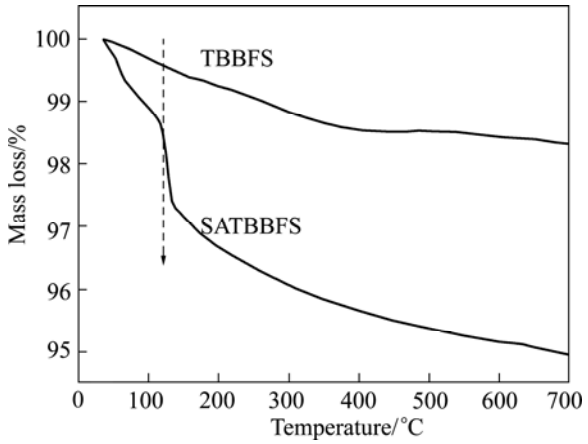

Fig.5 TGA curves of TBBFS and SATBBFS catalyst

is attributed to the evaporation of crystallization water and further decomposition/desorption of SO_4^{2-} species on the surface of SATBBFS catalyst at high temperature[13]. In addition, the contents of undecomposed SO_4^{2-} are 2.11% for $SATBBFS_{400}$, 1.84% for $SATBBFS_{500}$, 1.73% for $SATBBFS_{600}$ and 1.63% for $SATBBFS_{700}$, respectively.

3.4 Adsorption capacity

The adsorption capacity of SATBBFS catalyst to Cr(VI) was evaluated by the adsorption amount. The higher adsorption amount corresponds to the stronger adsorption capacity of catalysts. Fig.6 shows the adsorption amounts of Cr(VI) on different catalysts. With the increase of calcination temperature, the adsorption capacity of catalysts decreases. It is noticeable that the adsorption amounts of Cr(VI) on SATBBFS catalysts are all higher than those on TBBFS catalyst and reaches the highest values at calcination temperature of 400 °C. Generally, the surface modification to catalyst should improve the chemical compatibility between catalyst and contamination to enhance the contamination adsorption on catalyst[14].

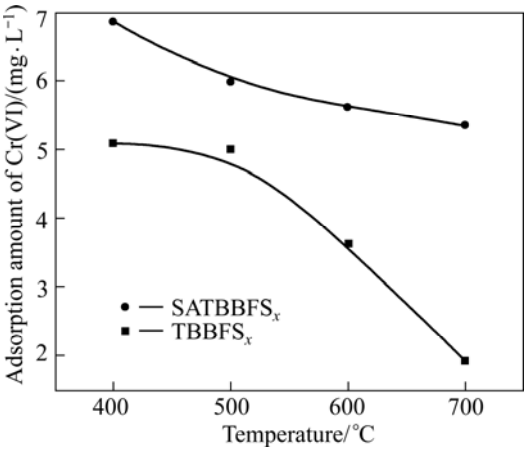

Fig.6 Adsorption amount of $TBBFS_x$ and $SATBBFS_x$ catalysts calcined at different temperatures

3.5 Photocatalytic activity

Based on the above analyses, it could be concluded that the sulfuric acid-modified TBBFS catalysts could not only make SATBBFS catalysts form the mixed phases($CaTiO_3/TiO_2$) but also enhance its adsorption capacity to Cr(VI). It has been found that there is a positive interaction for the formation of mixed phases, which enhances the electron–hole separation and then increases the total photocatalytic activity[12]. Therefore, SATBBFS catalysts may exhibit improved photocatalytic activity compared with TBBFS catalysts.

The photocatalytic performances of SATBBFS and TBBFS catalysts were evaluated with the photocatalytic reduction efficiency of Cr(VI) after 6 h irradiation under UV-visible light. To clearly compare the photocatalytic performances of various catalysts, the photocatalytic reduction efficiency of Cr(VI) in different $CaTiO_3$-to-TiO_2 mass ratio and photocatalysts are shown in Fig.7. From Fig.7 it can be seen that Cr(VI) shows a rapid reduction efficiency in the presence of $SATBBFS_{400}$ catalysts. And with the increase of the calcination temperature for SATBBFS catalysts, the reduction efficiency of Cr(VI) decreases slightly. In addition, the photocatalytic activity of $SATBBFS_{400}$ catalyst is still similar with that of $TBBFS_{700}$ catalyst. That may be caused by the steric hindrance effect, when the surface doping increases to a certain extent, the steric hindrance effect becomes obvious and holds back contamination adsorption on catalyst, and hence lowers the photocatalytic performance of catalyst[14]. It is generally thought that the photocatalytic performance depends on the phase structure, absorbance, and adsorption capacity of photocatalyst[14]. Due to higher ratio of $CaTiO_3$-to-TiO_2 and adsorption capacity of $SATBBFS_{400}$ catalyst than that of other catalysts, it is reasonable that $SATBBFS_{400}$ catalyst shows much better photocatalytic activity than others. Moreover, it is generally accepted that the acid environment of catalyst surface may markedly affect the Cr(VI) photoreduction[15−16]. Considering that marked desorption/decomposition of surface SO_4^{2-} was observed at calcination temperature higher than 100 °C (see Fig.5), the lower photocatalytic activities of SATBBFS catalysts calcined at higher temperature may also be ascribed to desorption of surface SO_4^{2-}. Consequently, the photocatalytic activities of SATBBFS catalysts are determined by the balanced result between adsorption capacity, multiphase structure and surface acidity.

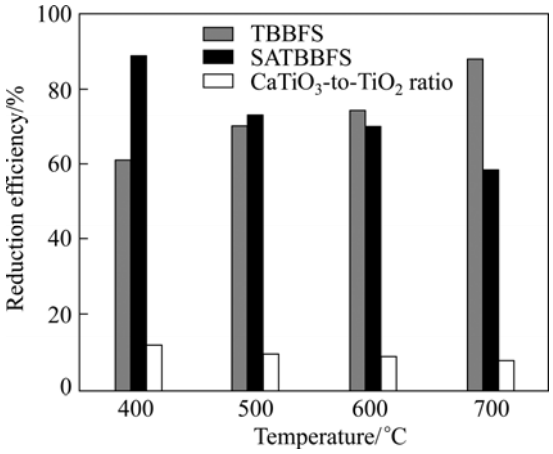

Fig.7 Photocatalytic reduction efficiency of Cr(VI) in different $CaTiO_3$-to-TiO_2 mass ratio and photocatalysts

3.6 Stability of catalysts

As a representative photocatalyst, $SATBBFS_{400}$ catalysts was investigated under UV-visible light

irradiation in Cr(VI) solution to study its recycled photocatalytic activity. It was found that third-recycled $SATBBFS_{400}$ catalyst still exhibited a photocatalytic activity similar to that of the fresh $SATBBFS_{400}$ catalyst. In addition, an examination to the separation performance of $SATBBFS_{400}$ catalyst and $P25TiO_2$ was carried out. The time for complete separation of $P25TiO_2$ and $SATBBFS_{400}$ catalysts requires 24 h and 130 h, respectively. Hence, $SATBBFS_{400}$ particles in suspension are easy to be handled and removed after their application in wastewater treatment. Based on the above results, the $SATBBFS_{400}$ is economical and effective photocatalyst for application in catalysis and separations.

4 Conclusions

1) Perovskite type $SATBBFS_x$ photocatalysts were prepared by a simple but powerful approach through the high energy ball milling method at different calcination temperatures.

2) For the photocatalytic reduction of Cr(VI), the photocatalytic activities of SATBBFS catalysts are found to be strongly dependent on $CaTiO_3$-to-TiO_2 ratio, adsorption capacity and surface acidity, and SATBBFS calcined at 400 °C shows a higher photocatalytic activity compared with other catalysts. Consequently, $SATBBFS_{400}$ photocatalyst is promising candidates for the photocatalytic reduction of Cr(VI) with high photocatalytic activity.

3) Based on our research results, effectively increasing $CaTiO_3$-to-TiO_2 ratio, adsorption capacity and surface acidity in $SATBBFS_{400}$ catalyst can be expected to further enhance its photocatalytic activity.

References

[1] LEI Xue-fei, XUE Xiang-xin. Photocatalytic reduction of Cr(VI) in Cr(VI)-acetic acid compound system [J]. The Chinese Journal of Process Engineering, 2008, 8(5): 901−907. (in Chinese)

[2] YANG He, XUE Xiang-xin, ZUO Liang, YANG Zhong-dong. Photocatalytic degradation of methylene blue with blast furnace slag containing Titanium [J]. The Chinese Journal of Process Engineering, 2004, 4(3): 265−268. (in Chinese)

[3] LEI X F, XUE X X. Preparation and characterization of perovskite type titania-bearing blast furnace slag photocatalyst [J]. Mat Sci Semicond Process, 2008, 11(4): 117−121.

[4] GUPTA V K, GUPTA M, SHARMA S. Process development for the removal of lead and chromium from aqueous solutions using red mud-an aluminium industry waste [J]. Water Res, 2001, 35(5):1125−1134.

[5] LEI Xue-fei, XUE Xiang-xin. Photocatalytic reduction of Cr(VI) in Cr(VI)-citric acid-ferric nitrate compound system [J]. The Chinese Journal of Nonferrous Metals, 2009, 19(2): 383−388. (in Chinese)

[6] SAMANTARAY S K, MOHAPATRA P, PARIDA K. Physico-chemical characterisation and photocatalytic activity of nanosized SO_4^{2-}/TiO_2 towards degradation of 4-nitrophenol [J]. J Mol Catal A Chem, 2003, 198(1/2): 277−287.

[7] JIANG F, ZHENG Z, XU Z Y, ZHENG S R, GUO Z B, CHEN L Q. Aqueous Cr(VI) photo-reduction catalyzed by TiO_2 and sulfated TiO_2 [J]. J Hazard Mater B, 2006, 134(1/3): 94−103.

[8] YU J G, WANG W G, CHENG B, SU B L. Enhancement of Photocatalytic activity of mesporous TiO_2 powders by hydrothermal surface fluorination treatment [J]. J Phys Chem C, 2009, 113(16): 6743−6750.

[9] LEI Xue-fei, XUE Xiang-xin. Effect of the different compound systems on photocatalytic reduction of Cr(VI) by titanium-bearing blast furnace slag [J]. Acta Chimica Sinica, 2009, 66(22): 2539−2546. (in Chinese)

[10] LEI X F, XUE X X. Preparation of perovskite type titanium-bearing blast furnace slag photocatalyst doped with sulphate and investigation on reduction Cr(VI) using UV-vis light [J]. Mater Chem Phys, 2008, 112(3): 928−933.

[11] PENG Wen-shi, LIU Gao-kui. Infrared spectra of inorganic and coordination compounds [M]. Beijing: Science Press, 1982. (in Chinese)

[12] YU J G, H YU G, CHENG B, ZHOU M H, ZHAO X J. Enhanced photocatalytic activity of TiO_2 powder (P25) by hydrothermal treatment [J]. J Mol Catal A Chem, 2006, 253(1/2): 112−118.

[13] COL´ON G, S´ANCHEZ-ESPANA J M, HIDALGO M. C. Effect of TiO_2 acidic pre-treatment on the photocatalytic properties for phenol degradation [J]. J Photochem Photobiol A, 2006, 179(1/2): 20−27.

[14] JIANG D, XU Y, WU D, SUN Y H. Visible-light responsive dye-modified TiO_2 photocatalyst [J]. J Solid State Chem, 2008, 181(3): 593−602.

[15] MOHAPATRA P, SAMANTARAY S K, PARIDA K. Photocatalytic reduction of hexavalent chromium in aqueous solution over sulphate modified titania [J]. J Photochem Photobiol A, 2005, 170(2): 189−194.

[16] PAPADAM T, XEKOUKOULOTAKIS N P, POULISO I, MANTZAVINOS D. Photocatalytic transformation of acid orange 20 and Cr(VI) in aqueous TiO_2 suspensions [J]. J Photochem Photobiol A, 2007, 186(2/3): 308−315.

(Edited by LI Xiang-qun)